Prussian Blue Nanoparticles | Hot Paper

DOI: 10.1002/anie.201310443

Nanosized Heterostructures of Au@Prussian Blue Analogues: Towards Multifunctionality at the Nanoscale**

Guillaume Maurin-Pasturel, Jérôme Long, Yannick Guari, Franck Godiard, Marc-Georg Willinger, Christian Guerin, and Joulia Larionova*

Abstract: *Access to multifunctionality at the nanoscale requires the development of hybrid nanostructures that combine materials of different natures. In this line of thought, current research on coordination polymers is not only focusing on their synthesis at the nanoscale, but also on combining these polymers with other materials. According to a novel and rational approach, single-layer Au@Prussian blue analogue (PBA) and double-layer Au@PBA@PBA′ core–shell nanoparticles (NPs) may be obtained through the growth of a cyano-bridged coordination network on the gold surface. The nanosized heterostructures combine the plasmonic optical properties of the gold core and the magnetic properties of the PBA shell. Whereas the single-layer nanoparticles are paramagnetic, the double-layer nanostructures display ferromagnetism; therefore, the overall structural motif may be considered as multifunctional. The developed synthetic concept also includes an easy access to hollow PBA NPs.*

Coordination polymer nanoparticles (NPs) are intriguing molecule-based nanosized materials that are made of metal ion nodes and molecular building blocks, and that have attracted a great deal of attention for the last decade. This interest is mainly due to many of the specific features that originate from the intrinsic molecular nature of these materials, such as definable and flexible molecular structures, porosity, low density, tunable physical and chemical properties, and soft-chemistry routes for their synthesis.[1] Moreover, because of their high surface-to-volume ratio, they possess unique size- and shape-dependent electrical, optical, magnetic, and catalytic properties that are strikingly different from those of their bulk counterparts. Different families of nanosized molecule-based materials, including metal–organic frameworks (MOFs),[2] infinite coordination polymers,[3] or cyano-bridged coordination polymers, which are also known as Prussian Blue and its analogues (PBAs),[4] have recently been investigated.

In this line of thought, current research on coordination polymers is not only focusing on their synthesis at the nanoscale, but also on combining these polymers with other materials. The design of such intricate materials in which the different chemical compositions meet at an interface constitutes a promising way towards multifunctional nanomaterials that combine multiple properties in a single system and exhibit diverse physical responses when subjected to various external stimuli.[5] These heterostructures can either feature a simple combination of the physical and chemical properties of the constitutive components or display novel properties that are due to the mutual interactions between the core and shell components. Numerous inorganic core–shell nanoparticles (NPs) with various properties or with properties that are superior to those of previously described nanoparticles have been reported.[6] For example, semiconductor@semiconductor[7] and metal@semiconductor nanocrystals[8] with tuned optical properties, metal@metal,[9] metal@metal oxide, and metal oxide@metal nanoobjects with advanced catalytic, optical, and magneto-plasmonic properties,[10] and metal or metal oxide@silica NPs, which have been proposed as multifunctional platforms for a variety of applications, have been described.[11] On the other hand, examples of heterostructures with a coordination polymer component remain relatively scarce.

Several heterostructured systems that combine inorganic materials with coordination polymers or MOFs have been investigated because of their enhanced catalytic activity or because of an association of the magnetic or optical properties of the inorganic NPs with the porosity and the electrochemical or magnetic properties of the coordination polymers.[5,12] In most cases, multiple metal (Au, Pt, Ag, Pd, Ru, Cu, Ni),[13] metal oxide (Fe_3O_4),[14] or quantum dot (CdTe, ZnO)[15] NPs were embedded in various porous MOF matrices to yield micro- or nanosized hybrid systems. Among these inorganic cores, gold NPs are particularly appropriate for the design of multifunctional systems owing to their catalytic properties and the optical features that arise from the surface plasmon band. Examples of nano-heterostructures with a gold core include gold NPs that are decorated with a MOF ($MOF = Zn_4O(BDC)_3$, $BDC = 1,4$-benzenedicarboxylate) and selectively entrap CO_2[16] and gold NPs that are encapsulated by a MIL-100(Fe)[17] or ZIF-8

[*] G. Maurin-Pasturel, Dr. J. Long, Dr. Y. Guari, Prof. Dr. C. Guerin, Prof. Dr. J. Larionova
Institut Charles Gerhardt Montpellier
UMR 5253 CNRS-UM2-ENSCM-UM1
Equipe Chimie Moléculaire et Organisation du Solide
Université Montpellier 2
Place Eugène Bataillon, 34095 Montpellier Cedex 5 (France)
E-mail: yannick.guari@um2.fr
F. Godiard
Service de microscopie électronique
Université Montpellier 2
Place Eugène Bataillon, 34095 Montpellier Cedex 5 (France)
Dr. M.-G. Willinger
Fritz Haber Institute of the Max Planck Society
Department of Inorganic Chemistry
Faradayweg 4-6, 14195 Berlin (Germany)

[**] We thank UM2, CNRS, and PAC ICGM.

Supporting information for this article is available on the WWW under http://dx.doi.org/10.1002/anie.201310443.

(Zn^{2+}-based imidazolate framework) shell,[18] which display enhanced catalytic activity because of synergistic effects. However, to the best of our knowledge, the design of core–shell heterostructures of a single inorganic NP that is coated with a uniform and well-defined layer of coordination polymer to give strictly individual core–shell heterostructures at the nanoscale has not been described. Herein, we report a new and rational approach for the design of single- and double-layer multifunctional magneto-optical Au@PBA heterostructures of uniform shape that have a coordination polymer shell of tunable thickness and exhibit the characteristic surface plasmon band of the gold core and the magnetic properties of the PBA shell. Remarkably, the gold core can be removed postsynthetically to give hollow PBA nanostructures.

The single-layer Au@PBA heterostructures were obtained by a two-step approach that consists of 1) the synthesis of cyanide-stabilized gold NPs in water through reduction of the dicyanoaurate precursor $[Au(CN)_2]^-$ with potassium borohydride[19] and 2) the subsequent time-controlled growth of the cyano-bridged coordination polymer shell on the surface of these gold NPs (Figure 1, see also the Supporting Information). The reaction between $[Au(CN)_2]^-$ and KBH_4 in water led to the appearance of a characteristic red color, which indicates the formation of gold NPs. After 20 minutes, the cyano-bridged coordination shell could be grown by the simultaneous addition of two aqueous solutions of the respective molecular precursors, $K_3[Fe^{III}(CN)_6]$ and $Ni^{II}Cl_2{\cdot}6H_2O$. Control of the rate of precursor addition

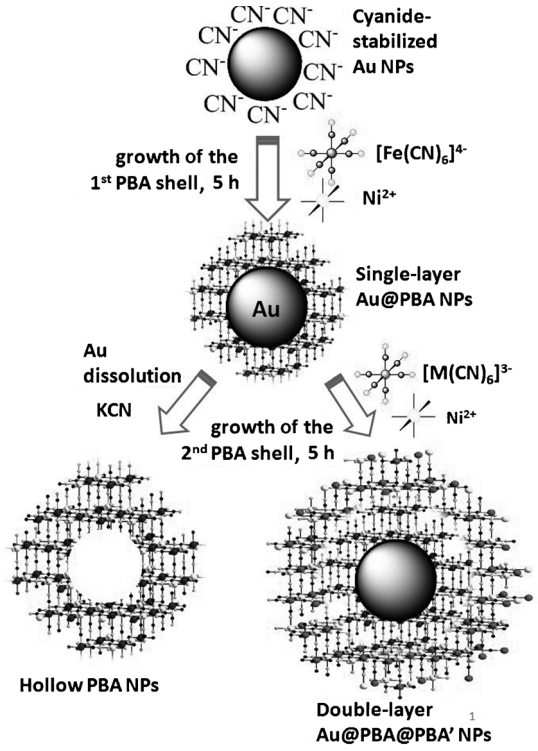

Figure 1. Schematic representations of single-layer Au@PBA NPs, double-layer Au@PBA@PBA′ core–shell NPs, and hollow PBA NPs that were obtained through the growth of a cyano-bridged coordination network on the gold surface.

($2\,mL\,h^{-1}$) is essential to foster growth of the cyano-bridged network at the surface of the gold NPs rather than self-nucleation. After complete addition (5 h), the obtained single-layer $Au@KNi^{II}[Fe^{II}(CN)_6]$ (Au@KNiFe) NPs were recovered by centrifugation and washed with water and ethanol. Their infrared (IR) spectrum confirmed the formation of the cyano-bridged network, as a single broad band at $2094\,cm^{-1}$ was observed in the cyanide stretching region, which is characteristic of the Fe^{II}–CN–Ni^{II} linkage (Supporting Information, Figure S1).[20] It clearly indicates that the $[Fe^{III}(CN)_6]^{3-}$ cyanometallate moiety was reduced to $[Fe^{II}(CN)_6]^{4-}$ during the shell-growth process because of the presence of the borohydride. The composition of the nanoparticles was determined by elemental analysis to be $Au_{1.08}@K_{1.20}Ni^{II}[Fe^{II}(CN)_6]_{0.80}$. Magnetic measurements support the total reduction of the cyanometallate moiety, as the Au@KNiFe NPs behaved as a paramagnetic compound with interactions between the Ni^{2+} ions through the diamagnetic $[Fe^{II}(CN)_6]^{4-}$ moiety at low temperature (Figure S2).

A powder X-ray diffraction (PXRD) pattern corroborated the formation of the targeted heterostructure (Figure S3). Diffraction peaks that are characteristic of the *fcc* gold metal structure (00-004-0784) are observed at 38.2, 44.4, 64.7, and 77.7° and are indexed in the space group *Fm*-3*m* with a cell parameter $a_{gold} = 4.08$ Å. The crystalline domain was calculated from the Scherrer formula, which gave an average value of approximately 15 nm. Furthermore, the PXRD pattern exhibited peaks that are characteristic of the *fcc* structure of $Ni^{II}_2[Fe^{II}(CN)_6]$, which were indexed in the *F4-3m* (01-075-0037) space group with a cell parameter of $a_{NiFe} = 10.07$ Å and a crystalline domain size of approximately 26 nm (d_{200} reflection).

Results from transmission electron microscopy (TEM) and high resolution transmission electron microscopy (HRTEM) indicate that the obtained NPs present well-defined core–shell structures of uniform size and shape (Figure 2; see also Figure S4). The gold cores have a mean diameter of 19.5 ± 4.3 nm, which is consistent with the value obtained from PXRD. Each single core is coated by a coordination polymer shell, which results in core–shell NPs with an overall diameter of 52.4 ± 8.6 nm. Selected area electron diffraction on individual nanoparticles confirmed the presence of crystalline phases of both $K_{1.20}Ni^{II}[Fe^{II}(CN)_6]_{0.80}$ and gold (Figure S5).

To determine the mechanism of the shell growth on the gold surface, $K_{1.20}Ni^{II}[Fe^{II}(CN)_6]_{0.80}$ shell formation was followed in real time by TEM. A series of TEM images that were taken during PBA shell growth revealed a regular increase in thickness for a reaction time from 20 minutes to five hours (Figures S6 and S7). The size of the gold core remained the same during the shell growth. It is therefore reasonable to presume that the formation of the PBA shell occurs by coordination of the Ni^{2+} and/or ferrocyanide moieties to the gold surface at the beginning of the growth process rather than during a postsynthetic redistribution of the negatively charged PBA NPs on the gold surface. Performing the same reaction with $HAuCl_4$ as the gold precursor did not yield the targeted heterostructures, which indicates that cyanide mol-

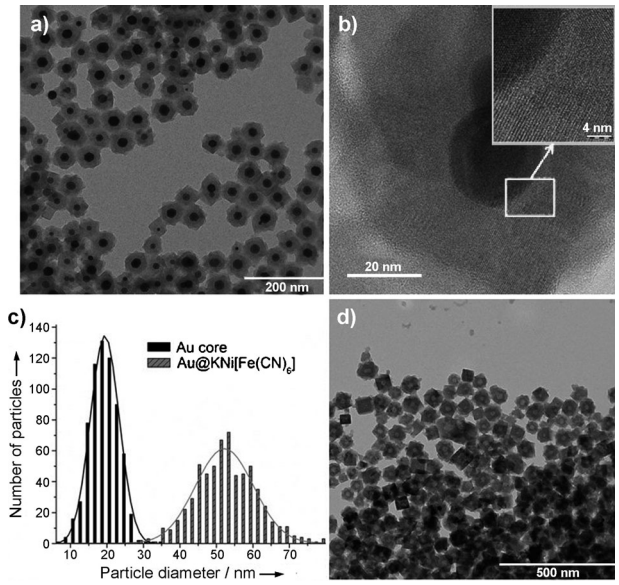

Figure 2. a, b) TEM (a) and HRTEM (b) images of the Au@KNiFe NPs. c) Corresponding histograms of the size distributions for the gold core and the overall diameter. d) TEM image of the hollow $KNi[Fe(CN)_6]$ NPs.

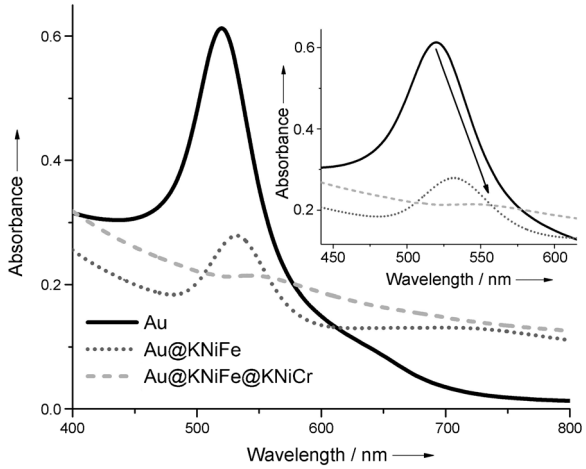

Figure 3. Electronic spectra of Au, Au@KNiFe, Au@KNiFe@KNiCr NPs in the visible region. Inset: magnified image of the surface plasmon band of the gold centers.

ecules play a decisive role in directing the growth of the PBA shell.

The optical properties of the uncoated gold NPs include an intense surface plasmon absorption band in the visible region at 520 nm (Figure 3).[21] The exact position and width of this band are extremely sensitive to any perturbation of the gold surface[22] and, by extension, to the presence of a PBA shell. The refractive index of the cyano-bridged coordination polymer shell is different from that of the gold and the surrounding water. As the gold NPs are covered with $K_{1.20}Ni^{II}[Fe^{II}(CN)_6]_{0.80}$, the surface plasmon band is red-shifted to $\lambda_{max} = 533$ nm (Figure 3), as predicted by the Mie theory and observed for gold NPs coated with a relatively thin (< 60 nm) layer of silica,[23] ZrO_2, or TiO_2.[24] This finding is explained by an increase in the local refractive index around the gold NPs.

It is well known that the gold NPs are subjected to an etching process in the presence of cyanide and oxygen because of the high stability constant of the gold cyanide complex $[Au(CN)_2]^-$ ($10^{37}\,M^{-2}$).[25] Owing to the intrinsic porosity of the PBA network, hollow PBA NPs can be obtained by simply dispersing the core–shell Au@KNiFe NPs in a KCN solution (10^{-3} M; Figure 1). This reaction induced the disappearance of the red color, which implies the dissolution of the gold cores through the pores of the PBA shell and the formation of colorless hollow PBA NPs and gold cyanide complexes $[Au(CN)_2]^-$ in solution.[19] The etching reaction was monitored by electronic spectroscopy; the surface plasmon band had vanished after 23 hours, indicating complete core dissolution (Figure S8). The integrity of the cyano-bridged $K_{1.20}Ni^{II}[Fe^{II}(CN)_6]_{0.80}$ network of the isolated hollow NPs was confirmed by IR spectroscopy and the presence of the characteristic band at 2094 cm^{-1} (Figure S9). TEM analysis of these NPs revealed the formation of hollow nanoobjects with a mean size of 53.8 ± 5.2 nm, which is close to the size of the initial core–shell NPs (Figure 2d). To date, only one effective method for the preparation of crystalline hollow PBA nanoparticles by etching with HCl under hydrothermal conditions has been described.[26]

Multifunctional double-layer Au@PBA@PBA′ heterostructures with both plasmonic and magnetic properties may be obtained from the single-layer Au@PBA NPs by growing a second ferromagnetic shell (Figure S10 and S11). The possibility of epitaxial growth of a cyano-bridged coordination polymer on the surface of another cyano-bridged coordination polymer with closed cell parameters has already been demonstrated with surfactant-free core NPs.[27] Pursuing this line of thought, the single-layer Au@KNiFe NPs were further reacted with $K_3[Cr^{III}(CN)_6]$ and $Ni^{II}Cl_2{\cdot}6H_2O$ under the conditions that also led to the formation of the first shell for the design of $Au@KNi^{II}[Fe^{II}(CN)_6]@KNi^{II}[Cr^{III}(CN)_6]$ (Au@KNiFe@KNiCr) NPs (Figure 1). Aside from the cyanide stretching vibration at 2090 cm^{-1} that is characteristic of the first Fe^{II}–CN–Ni^{II} layer, an additional Cr^{III}–CN–Ni^{II} stretching vibration at 2172 cm^{-1} was observed by IR spectroscopy (Figure S12). The PXRD pattern also showed two sets of distinct peaks, which confirmed the presence of the $KNi^{II}[Fe^{II}(CN)_6]$ and $KNi^{II}[Cr^{III}(CN)_6]$ shells in accordance with the significant difference in the relative cell parameters, which were determined to be $a_{NiCr} = 10.46$ Å and $a_{NiFe} = 10.07$ Å (Figure S3). TEM confirmed the subsequent growth of a second PBA shell (Figure S13), revealing the presence of NPs that are uniform in size and shape with a mean size of the gold core of 20.6 ± 3.2 nm and an average overall diameter of 133.3 ± 11.5 nm. EDS mapping was carried out to confirm the growth of the second layer (Figure S14). The distributions of iron and chromium were thus elucidated, the latter being present in the second layer at the periphery of the NPs, which indicates that no redistribution and mixing of the PBA phases between the different layers had occurred during the growth process.

The double-layer Au@KNiFe@KNiCr NPs feature both the plasmonic properties of the gold core and the magnetic properties of the second cyano-bridged coordination polymer shell. The surface plasmon band was shifted to higher wavelengths (red shift; $\lambda_{max} = 545$ nm) in comparison with the single-shell NPs (Figure 3), which is consistent with the increase in shell thickness.[22] The presence of the second PBA shell induces an enlargement of the plasmon band, which may be explained by the confinement of the free electrons within the metal core.[24]

The magnetic properties of Au@KNiFe@KNiCr were studied using a SQUID-MPMS magnetometer that may be used for temperatures ranging from 1.8 K to 350 K and up to 7 T by applying the zero-field-cooled/field-cooled (ZFC/FC) magnetization method (Figure 4). The ZFC curve exhibited

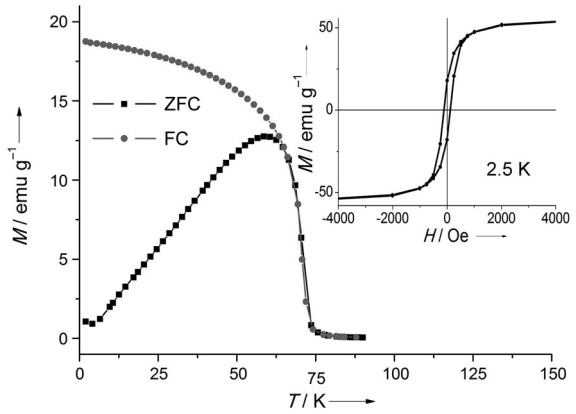

Figure 4. ZFC/FC magnetization curves for Au@KNiFe@KNiCr at an applied field of 100 Oe. Inset: hysteresis loop at 2.5 K.

a peak with a maximum at 60 K, which corresponds to the blocking temperature of the mean-size NPs, whereas the FC magnetization increases as the temperature decreases. The ZFC/FC curves start to diverge below 65 K, indicating a relatively narrow size distribution of the NPs. The field dependence of the magnetization measured at 2.5 K revealed the presence of a small hysteresis effect with a coercive field of 110 Oe, which confirmed the blocking of the magnetization. The values of both the blocking temperature and the coercive field are in accordance with the values that were previously obtained for $ANi[Cr(CN)_6]$ NPs (A = alkaline cation) with a diameter of greater than 20 nm.[28]

In summary, the described rational approach, which involves the growth of a cyano-bridged coordination polymer on the surface of gold NPs, appears to be promising for the design of core–shell nano-heterostructures with a single or multiple PBA shells as well as for the generation of hollow PBA nanoobjects. The former are well-defined core–shell structures with a single gold core and a single PBA shell in close interaction and constitutes the first example of such a hybrid heterostructure with PBA. These nanostructures combine the plasmonic optical properties of the gold core and the magnetic properties of the PBA shell. Whereas the single-layer materials display paramagnetism, the double-layer nanostructures are ferromagnetic; therefore, the overall structural motif may be considered as multifunctional. Moreover, the composition of the coordination polymer shell can be easily tailored by changing the metal ions, which induces a change of the magnetic properties. The extension of the simple synthetic procedure presented herein to other nanoscale heterostructures with various cyano-bridged coordination polymers with magnetic, host–guest, or optical properties opens new perspectives towards the design of multifunctional nanosystems that involve coordination polymers.

Received: December 2, 2013
Published online: February 26, 2014

Keywords: coordination networks · core–shell materials · gold nanoparticles · magnetic properties · Prussian blue nanoparticles

[1] M. Oh, C. A. Mirkin, *Nature* **2005**, *438*, 651.
[2] a) P. Horcajada, R. Gref, T. Baati, P. K. Allan, G. Maurin, P. Couvreur, G. Férey, R. E. Morris, C. Serre, *Chem. Rev.* **2012**, *112*, 1232; b) K. M. L. Taylor, A. Jin, W. Lin, *Angew. Chem.* **2008**, *120*, 7836; *Angew. Chem. Int. Ed.* **2008**, *47*, 7722.
[3] A. M. Spokoyny, D. Kim, A. Sumrein, C. A. Mirkin, *Chem. Soc. Rev.* **2009**, *38*, 1218.
[4] a) J. Larionova, Y. Guari, C. Sangregorio, C. Guérin, *New J. Chem.* **2009**, *33*, 1177; b) L. Catala, F. Volatron, D. Brinzei, T. Mallah, *Inorg. Chem.* **2009**, *48*, 3360; c) E. Dujardin, S. Mann, *Adv. Mater.* **2004**, *16*, 1125.
[5] a) S. B. Kim, C. Cai, S. Sun, D. A. Sweigart, *Angew. Chem.* **2009**, *121*, 2951; *Angew. Chem. Int. Ed.* **2009**, *48*, 2907; b) H.-L. Jiang, B. Liu, T. Akita, M. Haruta, H. Sakurai, Q. Xu, *J. Am. Chem. Soc.* **2009**, *131*, 11302; c) J. Son, H. J. Lee, M. Oh, *Chem. Eur. J.* **2013**, *19*, 6546; d) S. Hermes, M.-K. Schröter, R. Schmid, L. Khodeir, M. Muhler, A. Tissler, R. W. Fischer, R. A. Fischer, *Angew. Chem.* **2005**, *117*, 6394; *Angew. Chem. Int. Ed.* **2005**, *44*, 6237; e) H. J. Lee, W. Cho, M. Oh, *Chem. Commun.* **2012**, *48*, 221; f) C. Jo, H. J. Lee, M. Oh, *Adv. Mater.* **2011**, *23*, 1716.
[6] R. G. Chaudhuri, S. Paria, *Chem. Rev.* **2012**, *112*, 2373.
[7] For examples, see: a) P. Reiss, M. Protière, L. Li, *Small* **2009**, *5*, 154; b) Y. W. Cao, U. Banin, *J. Am. Chem. Soc.* **2000**, *122*, 9692; c) J. Wang, H. J. Han, *J. Colloid Interface Sci.* **2010**, *351*, 83; d) X. Peng, M. C. Schlamp, A. V. Kadavanich, A. P. Alivisatos, *J. Am. Chem. Soc.* **1997**, *119*, 7019; e) G. G. Yordanov, H. Yoshimura, C. D. Dushkin, *Colloid Polym. Sci.* **2008**, *286*, 1097; f) Y. Xia, Z. Tang, *Adv. Funct. Mater.* **2012**, *22*, 2585.
[8] a) R. Costi, A. E. Saunders, U. Banin, *Angew. Chem.* **2010**, *122*, 4996; *Angew. Chem. Int. Ed.* **2010**, *49*, 4878; b) J. T. Zhang, Y. Tang, K. Lee, M. Ouyang, *Science* **2010**, *327*, 1634; c) Y. Lei, W.-K. Chim, *J. Am. Chem. Soc.* **2005**, *127*, 1487; d) L. Zhang, D. A. Blom, H. Wang, *Chem. Mater.* **2011**, *23*, 4587; e) C. Gu, M. Park, C. Shannon, *Langmuir* **2009**, *25*, 410; f) Z. Sun, Z. Yang, J. Zhou, M. H. Yeung, W. H. Ni, H. Wu, J. F. Wang, *Angew. Chem.* **2009**, *121*, 2925; *Angew. Chem. Int. Ed.* **2009**, *48*, 2881.
[9] For examples, see: a) Y. W. Lee, M. Kim, Z. H. Kim, S. W. Han, *J. Am. Chem. Soc.* **2009**, *131*, 17036; b) F. Bao, J. F. Li, B. Ren, J. L. Yao, R. A. Gu, Z. Q. Tian, *J. Phys. Chem. C* **2008**, *112*, 345; c) X. B. Zhang, J. M. Yan, S. Han, H. Shioyama, Q. Xu, *J. Am. Chem. Soc.* **2009**, *131*, 2778; d) W. R. Lee, M. G. Kim, J. R. Choi, J.-I. Park, S. J. Ko, S. J. Oh, J. Cheon, *J. Am. Chem. Soc.* **2005**, *127*, 16090; e) J.-W. Hu, J.-F. Li, B. Ren, D.-Y. Wu, S.-G. Sun, Z.-Q. Tian, *J. Phys. Chem. C* **2007**, *111*, 1105; f) C. Li, Y. Yamauchi, *Phys. Chem. Chem. Phys.* **2013**, *15*, 3490.
[10] For examples, see: a) W. Shi, H. Zeng, Y. Sahoo, T. Y. Ohulchanskyy, Y. Ding, Z. L. Wang, P. N. Prasad, *Nano Lett.*

2006, *6*, 875; b) F. Pineider, C. de Julián Fernández, V. Videtta, E. Carlino, A. al Hourani, F. Wilhelm, A. Rogalev, P. D. Cozzoli, P. Ghigna, C. Sangregorio, *ACS Nano* **2013**, *7*, 857; c) K. C.-F. Leung, S. Xuan, X. Zhu, D. Wang, C.-P. Chak, S.-F. Lee, W. K.-W. Ho, B. C.-T. Chung, *Chem. Soc. Rev.* **2012**, *41*, 1911; d) Y. Yin, R. M. Rioux, C. K. Erdonmez, S. Hughes, G. A. Somorjai, A. P. Alivisatos, *Science* **2004**, *304*, 711; e) C. Levin, C. Hofmann, T. A. Ali, A. T. Kelly, E. Morosan, P. Nordlander, K. H. Whitmire, N. J. Halas, *ACS Nano* **2009**, *3*, 1379; f) J. Du, J. Qi, D. Wang, Z. Tang, *Energy Environ. Sci.* **2012**, *5*, 6914.

[11] For examples, see: a) F. Mazaleyrat, M. Ammar, M. LoBue, J. P. Bonnet, P. Audebert, G. Y. Wang, Y. Champion, M. Hytch, E. J. Snoeck, *J. Alloys Compd.* **2009**, *483*, 473; b) J. Lee, Y. Lee, J. K. Youn, H. B. Na, T. Yu, H. Kim, S. M. Lee, Y. M. Koo, J. H. Kwak, H. Park, H. N. Chang, M. Hwang, J. G. Park, J. Kim, T. Hyeon, *Small* **2008**, *4*, 143; c) F. G. Aliev, M. A. Correa-Duarte, A. Mamedov, J. W. Ostrander, M. Giersig, L. M. Liz-Marzan, N. A. Kotov, *Adv. Mater.* **1999**, *11*, 1006.

[12] Y. Liu, Z. Tang, *Adv. Mater.* **2013**, *25*, 5819.

[13] a) J.-D. Qiu, H.-Z. Peng, R.-P. Liang, J. Li, X.-H. Xia, *Langmuir* **2007**, *23*, 2133; b) K. Liu, R. Yuan, Y. Chai, D. Tang, H. An, *Bioprocess Biosyst. Eng.* **2010**, *33*, 179; c) Z. Chu, Y. Zhang, X. Dong, W. Jin, N. Xu, B. Tieke, *J. Mater. Chem.* **2010**, *20*, 7815; d) C. Wang, S. Chen, Y. Xiang, W. Li, X. Zhong, X. Che, J. Li, *J. Mol. Catal. B* **2011**, *69*, 1; e) Y. Namiki, T. Namiki, Y. Ishii, S. Koido, Y. Nagase, A. Tsubota, N. Tada, Y. Katamoto, *Pharm. Res.* **2012**, *29*, 1404; f) L. Jin, Y. Fang, L. Shang, Y. Liu, J. Li, L. Wang, P. Hu, S. Dong, *Chem. Commun.* **2013**, *49*, 243.

[14] F. Ke, L.-G. Qiu, Y.-P. Yuan, X. Jiang, J.-F. Zhu, *J. Mater. Chem.* **2012**, *22*, 9497.

[15] a) P. L. Feng, J. J. Perry IV, S. Nikodemski, B. W. Jacobs, S. T. Meek, M. D. Allendorf, *J. Am. Chem. Soc.* **2010**, *132*, 15487.

[16] L. He, Y. Liu, J. Liu, Y. Xiong, J. Zheng, Y. Liu, Z. Tang, *Angew. Chem.* **2013**, *125*, 3829 – 3833; *Angew. Chem. Int. Ed.* **2013**, *52*, 3741 – 3745.

[17] F. Ke, J. Zhu, L.-G. Qiu, X. Jiang, *Chem. Commun.* **2013**, *49*, 1267.

[18] G. Lu, S. Z. Li, Z. Guo, O. K. Farha, B. G. Hauser, X. Y. Qi, Y. Wang, X. Wang, S. Y. Han, X. G. Liu, J. S. DuChene, H. Zhang, Q. C. Zhang, X. D. Chen, J. Ma, S. C. J. Loo, W. D. Wei, Y. H. Yang, J. T. Hupp, F. W. Huo, *Nat. Chem.* **2012**, *4*, 310.

[19] C.-C. Huang, W.-C. Lai, C.-Y. Tsai, C.-H. Yang, C.-S. Yeh, *Chem. Eur. J.* **2012**, *18*, 4107.

[20] a) O. Sato, *J. Solid State Electrochem.* **2007**, *11*, 773; b) O. N. Risset, E. S. Knowles, S. Ma, M. W. Meisel, D. R. Talham, *Chem. Mater.* **2013**, *25*, 42.

[21] For an example, see: C. J. Murphy, A. M. Gole, S. E. Hunyadi, C. J. Orendorff, *Inorg. Chem.* **2006**, *45*, 7544.

[22] a) K. M. Mayer, J. H. Hafner, *Chem. Rev.* **2011**, *111*, 3828; b) J. Gong, F. Zhou, Z. Li, Z. Tang, *Langmuir* **2012**, *28*, 8959.

[23] L. M. Liz-Marzán, M. Giersig, P. Mulvaney, *Langmuir* **1996**, *12*, 4329.

[24] R. T. Tom, A. S. Nair, N. Singh, M. Aslam, C. L. Nagendra, R. Philip, K. Vijayamohanan, T. Pradeep, *Langmuir* **2003**, *19*, 3439.

[25] M. A. Rawashdeh-Omary, M. A. Omary, H. H. Patterson, *J. Am. Chem. Soc.* **2000**, *122*, 10371.

[26] a) M. Hu, S. Furukawa, R. Ohtani, H. Sukegawa, Y. Nemoto, J. Reboul, S. Kitagawa, Y. Yamauchi, *Angew. Chem.* **2012**, *124*, 1008; *Angew. Chem. Int. Ed.* **2012**, *51*, 984; b) M. Hu, N. L. Torad, Y. Yamauchi, *Eur. J. Inorg. Chem.* **2012**, 4795; c) M. Hu, A. A. Belik, M. Imura, Y. Yamuchi, *J. Am. Chem. Soc.* **2013**, *135*, 384.

[27] a) D. Asakura, C. H. Li, Y. Mizuno, M. Okubo, H. Zhou, D. R. Talham, *J. Am. Chem. Soc.* **2013**, *135*, 2793; b) M. F. Dumont, E. S. Knowles, A. Guiet, D. M. Pajerowski, A. Gomez, S. W. Kycia, M. W. Meisel, D. R. Talham, *Inorg. Chem.* **2011**, *50*, 4295; c) L. Catala, D. Brinzei, Y. Prado, A. Gloter, O. Stéphan, G. Rogez, T. Mallah, *Angew. Chem.* **2009**, *121*, 189; *Angew. Chem. Int. Ed.* **2009**, *48*, 183; d) Y. Prado, N. Dia, L. Lisnard, G. Rogez, F. Brisset, L. Catala, T. Mallah, *Chem. Commun.* **2012**, *48*, 11455; e) M. Presle, J. Lemainque, J.-M. Guigner, E. Larquet, I. Maurin, J.-P. Boilot, T. Gacoin, *New J. Chem.* **2011**, *35*, 1296.

[28] Y. Prado, L. Lisnard, D. Heurtaux, G. Rogez, A. Gloter, O. Stéphan, N. Dia, E. Rivière, L. Catala, T. Mallah, *Chem. Commun.* **2011**, *47*, 1051.

